Interferon Induced Transmembrane Protein 3 (IFITM3) Restricts PRRSV Replication via Post-Entry Mechanisms

Pratik Katwal , Shamiq Aftab , Eric Nelson , Michael Hildreth , Shitao Li , Xiuqing Wang *

Posted Date: 9 June 2025

doi: 10.20944/preprints202506.0696.v1

Keywords: virus restriction factors; interferon stimulated genes (ISGs); Interferon induced trans-membrane protein 3 (IFITM3); Porcine Reproductive and Respiratory Syndrome Virus (PRRSV)

 doi:10.20944/preprints202506.0696.v1

Article

Interferon Induced Transmembrane Protein 3 (IFITM3) Restricts PRRSV Replication via Post-Entry Mechanisms

Pratik Katwal [1], Shamiq Aftab [1], Eric Nelson [2], Michael Hildreth [1], Shitao Li [3] and Xiuqing Wang [1,*]

[1] Department of Biology and Microbiology, South Dakota State University, Brookings, SD, 57007, USA; pratiksagarmatha@outlook.com; shamiq.aftab@sanfordhealth.org; michael.hildreth@sdstate.edu

[2] Department of Veterinary and Biomedical Sciences, South Dakota State University, Brookings, SD, 57007, USA; eric.nelson@sdstate.edu

[3] Department of Microbiology and Immunology, Tulane University, New Orleans, LA 70112, USA; sli38@tulane.edu

* Correspondence: xiuqing.wang@sdstate.edu

Abstract: Interferon induced transmembrane protein 3 (IFITM3) is a member of the family of interferon stimulated genes (ISGs) that inhibits a diverse array of enveloped viruses which enter host cells by endocytosis. Porcine reproductive and respiratory syndrome virus (PRRSV) is an enveloped RNA virus causing significant economic losses to the swine industry. Very little is known as to how IFITM3 restricts PRRSV. In this study, the role of IFITM3 in PRRSV infection was studied *in vitro* using MARC-145 cells. IFITM3 overexpression reduced PRRSV replication, while siRNA induced knockdown of endogenous IFITM3 increased PRRSV RNA copies and virus titers. Colocalization of virus with IFITM3 was observed at both 3 and 24 hours post infection (hpi). Quantitative analysis of confocal microscopic images showed that an average of 73% of IFITM3 expressing cells were stained positive for PRRSV at 3 hpi, while only an average of 27% of IFITM3 expressing cells were stained positive for PRRSV at 24 hpi. These findings suggest that IFITM3 may restrict PRRSV at the post-entry steps. Future studies are needed to better understand the mechanisms by which this restriction factor inhibits PRRSV.

Keywords: virus restriction factors; interferon stimulated genes (ISGs); Interferon induced transmembrane protein 3 (IFITM3); Porcine Reproductive and Respiratory Syndrome Virus (PRRSV)

1. Introduction

Restriction factors function to antagonize virus infection and can target viruses at various stages of their life cycle. Some block cytosolic entry of enveloped viruses by either directly inhibiting virus fusion at the cell surface or by preventing fusion within the endosomes [1]. The Interferon induced transmembrane proteins (IFITMs) belong to a class of interferon stimulated genes (ISGs) and are constitutively expressed in various cell types and potently induced upon interferon treatment [2,3]. Of the five known members of the IFITM family, IFITM1, 2, and 3 are antiviral restriction factors and inhibit viruses that either enter by direct fusion with the cell membrane (IFITM1), or by endosomal trafficking (IFITM2 and IFITM3) [4,5]. IFITM3 also inhibits virus-host membrane fusion within the endosomes [6]. Other well-studied classical ISGs such as Mx1, OAS, and PKR also play important role in restricting virus replication [7–9].

The role of IFITM3 in Influenza A virus (IAV) infection has been well studied [10]. IFITM3 knockout mouse embryonic fibroblasts (MEFs) are highly susceptible to IAV infection [11]. The cytosolic release of the IAV viral ribonucleoproteins (vRNPs) is restricted by IFITM3, thereby blocking their subsequent nuclear entry [2,6]. Enveloped viruses such as IAV that are pH sensitive

 doi:10.20944/preprints202506.0696.v1

and require low pH for fusion are highly restricted by IFITM3 [12]. The IFITM3 protein is expressed in the early or late endosomes and strongly inhibits viruses that enter through late endosomes. Overall, the block to virus uncoating results in the trapping of viruses in the acidic endolysosomes within which it undergoes degradation [2]. IFITM3 expression has been shown to expand acidified endosomes as evident from colocalization with endosomal markers, chiefly Rab7 and LAMP-1 [2]. Other viruses such as West Nile virus, Vesicular stomatitis virus, etc. that fuse at pH greater than 6 are also inhibited by IFITM3 [13,14]. IFITM3 proteins inhibit a broad spectrum of enveloped RNA viruses [5,13]. Recently, IFITM3 has also been shown to restrict Zika virus, an important emerging pathogen [15].

Porcine reproductive and respiratory syndrome virus (PRRSV) is an enveloped, positive sense, and single stranded RNA virus. It is a highly pathogenic virus that mainly causes respiratory disease in newborn pigs and reproductive disease in sows [16]. PRRSV belongs to the order *Nidovirales* within the family *Arteriviridae* [16]. Upon initial attachment and internalization via binding to the sialoadhesin molecules, PRRSV enters into early endosome through a clathrin-dependent pathway in clathrin coated vesicles and is dependent on its binding to the CD163 receptor [17,18]. CD163 functions as the principal PRRSV receptor that recycles between plasma membrane and endosomes [18–20]. PRRSV is known to enter cells through the endocytic pathway [17,21]. However, one study showed that PRRSV does not appear to be associated with later endosome/lysosomes [22].

The impact of many ISGs including IFITM3 on PRRSV replication has not been extensively studied. One recent study has reported the antiviral role of IFITM3 on PRRSV infection [23]. Zhang et al. showed that IFITM3 did not block PRRSV entry into endosome or lysosome, but restricted PRRSV fusion through cholesterol accumulation within endosomal membrane [23]. These authors have further suggested that IFITM3 is incorporated into PRRSV virions, which results in reduced infectivity and cell-cell spread of PRRSV [24]. Our previous study suggested that ZMPSTE24, the downstream effector of IFITM3, restricts PRRSV replication at post-entry steps [25]. Here in this study, we have examined the role of IFITM3 in PRRSV replication in MARC-145 cells. Our data suggested that IFITM3 did not impact virus entry, but restricted PRRSV replication at post-entry steps.

2. Materials and Methods

2.1. IFITM3 Transfection in MARC-145 Cells

MARC-145 cells were cultured in a 12-well plate in DMEM medium supplemented with 10% FBS and 1% Penicillin-Streptomycin (complete DMEM medium). The 12-well plate was incubated in a humidified chamber at 37°C with 5% CO_2. After 24 h, cells were washed in DMEM medium and transfected with 1.25 μg of either the pQCXIP vector control (Q-series retroviral vector; Retro-X Q Vector Set) (Clontech, Cat. No. 631516; Takara Bio Inc.) or pQCXIP expressing the IFITM3-HA [11,26] in triplicate wells using lipofectamine 3000 Transfection kit (Invitrogen), following the manufacturer's protocol. The retroviral vector pQCXIP carries puromycin resistant gene and expresses IFITM3-HA, transfected in HEK293 packaging cells for stable expression [26]. Briefly, each plasmid DNA was diluted in DMEM medium with P3000 and mixed with Lipofectamine 3000 reagent. The transfection mix was then incubated at room temperature (RT) for 20 min after which 200 μl of the DNA-lipid complex was added dropwise to the respective wells. After incubation for 6 h at 37°C, the medium was replaced with complete DMEM medium. After 72 h, each of the six wells was infected with PRRSV 23983 at an MOI of 1 for 24 h. In some experiments, MARC-145 cells were treated with 1 μM of torin1 (Cell Signaling Technology, catalog# 14379) for 3 h. Then, cells together with supernatant were harvested. The supernatant and the pellets were stored separately at -80°C until used for further analysis.

Further, MARC-145 cells cultured in two 8-chamber slides (colocalization study) or a 96-well plate (cytotoxicity study) were transfected with 0.3 μg of either pQCXIP vector control or IFITM3-HA using lipofectamine 3000 reagent.

 doi:10.20944/preprints202506.0696.v1

Transfection in the 48-well plate was performed in two groups. In the first group, MARC-145 cells were transfected with 0.3 µg of either pQCXIP plasmid vector or pQCXIP IFITM3-HA in triplicates using lipofectamine 3000 reagent. The second group was transfected following same transfection scheme (Amphotericin B treatment group).

2.2. siRNA Induced Knockdown of IFITM3 in MARC-145 Cells

MARC-145 cells were cultured in a 12-well plate. Following 24 h incubation at 37 °C, cells were transfected with either negative control siRNA (Ambion, cat. no. AM4642) or IFITM3 siRNA (Life technologies, siRNA ID#s195035) at a final concentration of 40 nM per well using Lipofectamine RNAi max reagent (Invitrogen) according to the manufacturer's protocol. Transfection was performed in triplicate wells. The siRNA was mixed with RNAi max reagent diluted in DMEM medium in 1:1 ratio. The mixture was incubated at RT for 5 min after which 125 µl of the siRNA complex was added dropwise to the respective wells of MARC-145 cells in DMEM medium. The 12-well plate was then incubated at 37°C for 6 h. Then the DMEM medium was replaced with complete DMEM growth medium and incubated for 72 h. Next, the cells in each well of the 12-well plate were infected with PRRSV 23983 at an MOI of 1 for 24 h after which cells were scraped and harvested with supernatant. Following centrifugation, supernatant and cell pellets were separated and stored at -80°C

For the cytotoxicity experiment, 1.2 µl of either negative control siRNA or IFITM3 siRNA at a final concentration of 40 nM was used for transfection in triplicate wells of a 96-well plate. Thus 25 µl of transfection mix was added dropwise to the respective wells, then incubated at 37°C for 6 h and replaced with complete DMEM medium.

2.3. Western Blot Analysis

Cell pellets were resuspended with 60 µl cell lysis buffer (0.01M Tris-HCl pH 8, 0.14 M NaCl, 0.025% NaN3, 1% Triton x-100) treated with Halt™ protease and phosphatase inhibitor cocktail (Thermo Scientific, catalog# 78441) at 1:100 dilution. Each lysate sample thus obtained from overexpression of either the pQCXIP vector or the IFITM3-HA was vortexed for 15 s. The tubes were then incubated for 1 h at 4°C, with vortexing every 15 min. Each tube was then spun at 13,000 rpm for 1 min after which the lysate was transferred to a new tube. Next, 20 µl of each sample was mixed with equal volume of 2x western blot loading buffer (treated with beta-mercaptoethanol at 1:50 dilution). Each sample was incubated at 95°C for 5 min and then loaded into each well. Gels were run at 150 V for 1.5 h and then transferred to nitrocellulose membrane. Each membrane was incubated in blocking buffer (5% milk powder in 1x PBST or 5% BSA in 1x PBST) at room temperature (RT) for 1 h. Then the membranes were washed with 1x PBST and incubated by shaking overnight at 4°C with respective primary antibodies. The following primary antibodies were used: anti-HA mouse monoclonal 1o Ab (6E2) (Cell Signaling Technology, catalog# 2367) at 1:1000 dilution, anti-HA mouse monoclonal antibody (HA7) (Sigma Aldrich, catalog# H3663) at 1:5000 dilution, anti-PRRSV SR-30 1o monoclonal Ab (provided by Dr. Eric Nelson) at 1:300 dilution, anti-IFITM3 rabbit polyclonal antibody (Proteintech, catalog# 11714-1-AP) at 1:1000 dilution, anti-p-Akt (S743, Cell Signaling Technology, catalog# 9271S) at 1:1000 dilution, anti LC3B antibody (Sigma Aldrich, catalog# L7542) at 1:2000 dilution, and mouse monoclonal anti-beta actin Ab (Sigma-Aldrich, catalog# A2228) at 1:5000 dilution. Next day, the membrane was washed with 1x PBST three times and then incubated in dark at RT with Goat anti-Mouse IRDye® conjugated secondary Ab (LI-COR, catalog# 926-32210) diluted to 1:15,000. The membrane was washed and observed using LI-COR Odyssey Infrared Imaging System.

2.4. Interferon Stimulation of IFITM3 Gene in MARC-145 Cells

To study the dose dependent response of IFN-alpha treatment on IFITM3 gene expression, a 12-well plate was seeded with MARC-145 cells and incubated for 24 h at 37°C. Next, MARC-145 cells

 doi:10.20944/preprints202506.0696.v1

were treated with IFN-alpha at a concentration of either 50 U/ml, or 100 U/ml, or 500 U/ml in duplicate wells. Two wells were incubated with 1 ml of DMEM complete medium only (IFN-alpha untreated, control wells). After 12 h incubation, the medium was removed, and each well was infected with 1 MOI of PRRSV 23983 for 24 h at 37°C. Cells were then harvested, and the cell pellets were stored at -80°C for RT-PCR analysis of IFITM3 gene expression and PRRSV nucleocapsid (N) gene RNA copies.

2.5. Immunofluorescence Assay and Flow Cytometry

Amphotericin B at a concentration of 2.5 µg/ml was added to each of the six wells of a 48-well plate transfected with either vector control plasmid pQCXIP or IFITM3-HA in triplicates. Another set of six wells transfected similarly were not treated with Amphotericin B. After incubating the plate at 37°C for 1 h, Amphotericin B was removed. PRRSV 23983 was added at an MOI of 1 to all wells and the plate was incubated at 37°C for 24 h. Cells were then fixed with 80% acetone for 20 min at RT and air dried. Next, FITC conjugated anti-PRRSV Ab specific to N protein (SDOW-17) [27] at 1:80 dilution was added to each well and incubated at 37°C for 1 h. Cells were washed and observed using an Olympus IX70 Inverted-Microscope equipped with epi-fluorescence and phase contrast. Cells in each well were scraped, resuspended in PBS, and analyzed by flow cytometry for calculating mean fluorescence intensity of FITC staining.

2.6. Colocalization Study Using Confocal Microscopy

For the study of colocalization of PRRSV with endosomal markers, MARC-145 cells were cultured in three 8-chamber slides for each time point study. After 24 h, the cells were infected with PRRSV at a MOI of 10. Then at three time points -1 h, 3 h, or 6 h after infection, the cells were fixed with 3.8% formaldehyde for 10 min at RT, then washed in PBS for 5 min and treated with 0.2% Triton X-100 for 10 min, after which cells were again washed once and incubated with 5% goat serum in PBS (blocking buffer) for 1 h. Then cells were incubated with SDOW17 (FITC conjugated anti-PRRSV N) monoclonal Ab at 1:80 dilution, together with either anti-EEA1 Ab (Santa Cruz Biotechnology, sc-365652) or anti-Lamp-1 Ab (Santa Cruz Biotechnology, sc-19992) conjugated to Alexa Fluor 647. The cells were washed, then mounted using ProLong Gold antifade mounting reagent (Invitrogen) and observed with an Olympus Fluoview FV1200 Laser Scanning Confocal Microscope. For each time point, five random cells were selected and then with manual thresholding, the threshold range was selected to define the area of interest distinct from background [28]. The color (yellow) threshold was adjusted to measure the area of colocalized region (A1). Next, the threshold color was adjusted to select all five cells to obtain area of the total five cells (A2). The percentage colocalization was calculated by multiplying the fraction, (A1/A2) by 100. Mean percent colocalization was calculated for each time point from three selected areas (each with five cells).

MARC-145 cells cultured in two 8-chamber slides were transfected with either vector control pQCXIP or IFITM3-HA in duplicate wells of each slide as described earlier. For 3 h post infection (3 hpi) study, PRRSV 23983 at an MOI of 4 was added to all wells except one vector control transfected well. For 24 hpi study, cells were infected with PRRSV at an MOI of 1. After infecting cells with PRRSV for the respective times, the two slides were fixed using the protocol as described previously. Then the cells in each well were incubated overnight at RT with primary antibody diluted in 5% goat serum. Mouse monoclonal anti-HA primary antibody against HA tagged IFITM3 (6E2) (Cell Signaling Technology, cat. no. 2367) was added at a dilution of 1:1600 to all wells except the uninfected vector control transfected well to which 5% goat serum was added. Next day, the slides were washed three times with 1x PBS and then incubated for 1 h at 37°C with secondary antibody. To the three wells incubated with anti-Flag primary antibody, Alexa fluor 647 conjugated goat anti-mouse IgG secondary Ab (Abcam) at 1:200 dilution was added. After 1 h incubation, cells were washed and incubated with 1:80 diluted anti-PRRSV FITC conjugated Ab (SDOW17) at 37°C for 1 h. The uninfected vector control transfected well was incubated with Alexa fluor 647 secondary Ab only. The two slides were washed, counterstained with DAPI, and then mounted as described

 doi:10.20944/preprints202506.0696.v1

previously. The slides were then stored at 4°C overnight and observed with confocal microscopy to identify any colocalization between PRRSV and IFITM3 at 3 or 24 hpi. Five different microscopic fields at 40x magnification were analyzed for the pQCXIP vector control transfected group and IFITM3-HA transfected group. In each field, cells were counted by DAPI staining and then the percentage of cells staining for PRRSV (green) or IFITM3 (red) was calculated. Colocalization study was performed by counting the number of DAPI stained cells with yellow fluorescence which represents the overlap of the emission spectra for the green FITC and red Alexa fluor 647 signals. Uninfected control cells stained with FITC conjugated anti-PRRSV Ab were used as a control for comparing the background (green) staining with the PRRSV infected group.

2.7. Cytotoxicity Assay

MARC-145 cells cultured in a 96-well plate were transfected with either the pQCXIP vector control or pQCXIP encoding IFITM3-HA or negative control siRNA (Ambion, cat. no. AM4642) or IFITM3 siRNA (Life technologies, siRNA ID# s195035) in triplicate wells, as described earlier. After 72 h, each well incubated with 200 µl of DMEM growth medium was treated with 10 µl of Cell Counting Kit - 8 (CCK-80 solution, Sigma, cat. no. 96992) and incubated at 37°C for 3 h, after which absorbance was measured at 450 nm using a Synergy 2 plate reader (BioTek).

2.8. Real-Time Reverse Transcription PCR (RT-PCR)

Total RNA was extracted from cells using RNeasy Mini Kits (Qiagen cat. no. 74104) following the manufacturer's protocol. One µg of total RNA was reversed transcribed using a High-Capacity cDNA Reverse Transcription Kit (Applied Biosystems) under following reaction conditions: 25°C for 10 min, 37°C for 120 min, and 85°C for 5 min (Applied Biosystems GeneAmp PCR System 2400). Real time PCR was performed by using 3 µl of the cDNA for each reaction using Brilliant II SYBR Green QPCR master mix (Agilent Technologies). Forty cycles of following conditions were used: 95°C for 10 min, 95°C for 30 s, 55°C for 30 s, and 72°C for 30 s. Primers specific to beta-actin housekeeping gene, PRRSV N, IFITM3, and Mx1 are shown in Table 1. The reactions were run in a QuantStudio 6 Flex Real-Time PCR System (Applied Biosystems). Data analysis was performed by calculating the mean fold change in gene expression using the ΔΔCT method. Housekeeping gene beta-actin was used as a reference gene for comparing the fold change between two treatment groups [29].

Table 1. Primer sequences of IFITM3, PRRSV N, and the house-keeping gene (beta-actin).

Gene	Forward Primer (5′-3′)	(Reverse Primer (5′-3′)
beta-actin	TTGCTGACAGGATGCAGAAGGAGA	ACTCCTGCTTGCTGATCCACATCT
IFITM3	GGTCTTCGCTGGACACCAT	TGTCCCTAGACTTCACGGAGTA
PRRSV N	GTCAATCCAGACCGCCTTTA	GATCAGGCGCACAGTATGAT
Mx1	TTTTCAAGAAGGAGGCCAGCAA	TCAGGAACTTCCGCTTGTCG

2.9. TCID50 Titer

Fifty-percent tissue culture infectious dose ($TCID_{50}$) assay was performed to determine the infectious PRRSV 23983 titer in the supernatant at 24 hpi obtained from the previously described IFITM3 overexpression or siRNA induced knockdown experiments. TCID50 titer was determined using the Spearman-Karber method [21].

2.10. Statistical Analysis

A two tailed student's t-tests were used for all of comparisons, and p-values less than 0.05 ($p<0.05$) were considered significant.

 doi:10.20944/preprints202506.0696.v1

3. Results

3.1. Over-expression of exogenous IFITM3 reduces PRRSV replication

Western blotting analysis confirmed the expression of exogenous IFITM3 in cells transfected with plasmid containing IFITM3-HA (Figure 1a), but not in cells transfected with pQCXIP vector control (Figure 1a). Virus titers in the supernatants of cells harvested at 24 hpi showed an average of 5.4-fold decrease in IFITM3-HA transfected cells compared to vector controls ($p > 0.05$) (Figure 1b). Cytotoxicity assay showed that there were no significant differences in cell viability between vector control group and IFITM3 overexpressing group ($p > 0.05$) (Figure 1c). The mean absorbance values of vector control group and IFITM3 overexpressing group were 1.48 and 1.32 respectively (Figure 1c). These results suggest that overexpression of IFITM3 protein reduces PRRSV replication.

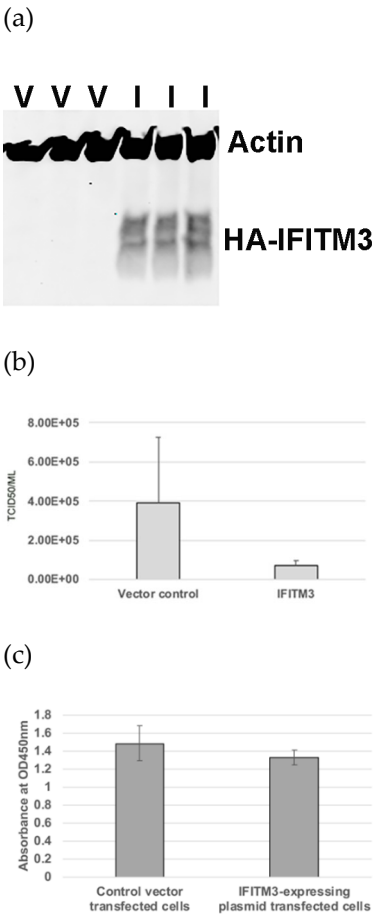

Figure 1. Over-expression of IFITM3 reduces PRRSV replication. (a) Western blotting analysis showing the expression of exogenous IFITM3 in cells transfected with plasmid containing IFITM3 (I), but not in cells transfected with vector control (V). (b) Virus titers in the supernatants of cells transfected with vector control or IFITM3 containing plasmid at 24 h after virus infection. An average of 5.4-fold decrease was observed in IFITM3 transfected cells compared to vector controls. (c) CCK-8 cytotoxicity assay was used to compare the difference in cell viability between QCXIP vector control and IFITM3-HA overexpressing MARC-145 cells. A p value < 0.05 was considered as statistically significant.

3.2. Knockdown of IFITM3 by siRNA Enhances PRRSV Replication

To validate the knockdown of endogenous IFITM3, qRT-PCR was performed to analyze the fold change in IFITM3 mRNA expression in IFITM3 silenced MARC-145 cells as compared to control silencing RNA. qRT-PCR confirmed the silencing of IFITM3, with an average of 50% knockdown efficiency (Figure 2a). qRT-PCR and $TCID_{50}$ assay were performed to quantify the viral RNA copies and supernatant virus titers in control silencing and IFITM3 silencing RNA transfected cells. An

 doi:10.20944/preprints202506.0696.v1

average of 1.28-fold increase in viral RNA copies ($p > 0.05$) and 1.22-fold increase in virus titers ($p > 0.05$) was observed in IFITM3 silencing RNA transfected cells compared to control silencing RNA transfected cells (Figure 2b,c). There were no significant differences ($p > 0.05$) in cell viability between control silencing RNA and IFITM3 silencing RNA (Figure 2d). The mean absorbance values of negative control silencing group and IFITM3 silencing group were 1.76 and 1.47 respectively (Figure 2d). This shows that knockdown of IFITM3 slightly enhanced virus replication.

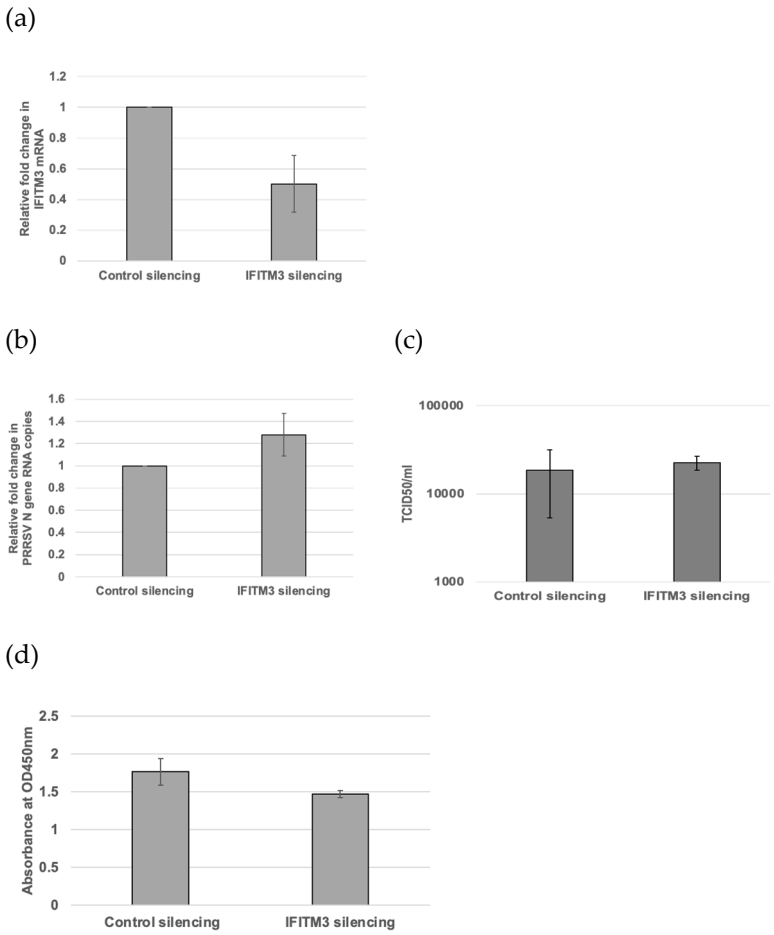

Figure 2. Silencing of IFITM3 slightly enhances PRRSV replication. (a) qRT-PCR showing the silencing of IFITM3. The averages and standard deviations of three replicates are shown. (b) qRT-PCR showing the viral RNA copies in control silencing and IFITM3 silencing RNA transfected cells. The averages and standard deviations of three replicates are shown. (c) A slightly enhanced $TCID_{50}$ virus titer (1.22-fold increase) in IFITM3 silencing RNA transfected cells compared to control silencing RNA transfected cells was observed. The averages and standard deviations of three replicates are shown. (d) Difference in cell viability was compared between the negative control siRNA and IFITM3 siRNA transfected MARC-145 cells. Graph shows mean absorbance values read at 450 nm between the two groups. A p value < 0.05 was considered as significant.

3.3. Inverse Correlation Between IFITM3 Expression Level and Virus Replication Efficiency

When compared to non-treated control group, PRRSV infection in MARC-145 cells upregulated the Mx1 gene expression but not IFITM3 (Figure 3a). IFN-alpha treatment induced the up-regulation of mRNA gene expression of both IFITM3 and Mx1 as compared to the control group (Figure 3a). At 50 U/ml IFN-alpha concentration, the mean fold change in IFITM3 gene expression as compared to IFN-alpha untreated cells was 1.94 (Figure 3b). At 100 U/ml concentration of IFN-alpha, the mean fold change in IFITM3 gene expression was 3.73 (Figure 3b). At 500 U/ml concentration of IFN-alpha, the mean fold change in IFITM3 expression was 4.91 (Figure 3b). A does dependent increase of IFITM3 mRNA level in IFN-alpha treated MARC-145 cells was detected. As compared to the IFN-alpha untreated group infected with PRRSV, the mean fold change in PRRSV N gene transcripts upon

 doi:10.20944/preprints202506.0696.v1

treatment with IFN alpha at 50 U/ml, 100 U/ml, and 500 U/ml were 0.34, 0.16, and 0.07 respectively (Figure 3b). A dose dependent decrease in PRRSV gene transcript in IFN-alpha treated MARC-145 cells was observed. These results showed an inverse correlation between IFITM3 expression and PRRSV replication in IFN-alpha treated MARC-145 cells.

Western blotting analysis showed that IFITM3 over-expression increased total IFITM3 protein by 6.2-fold when compared to endogenous IFITM3 level (Figure 3c). Accordingly, no virus was detected in cells over-expressing IFITM3 by $TCID_{50}$ assay, while cells only expressing endogenous level of IFITM3 had a virus titer of $1.9x10^4$/ml (Figure 3d). These data further confirm the inverse correlation between IFITM3 expression level and virus replication efficiency.

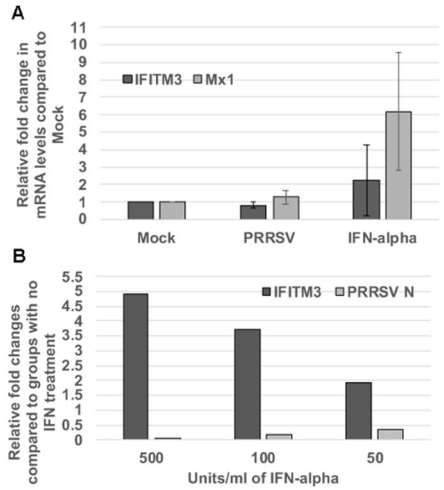

(c)

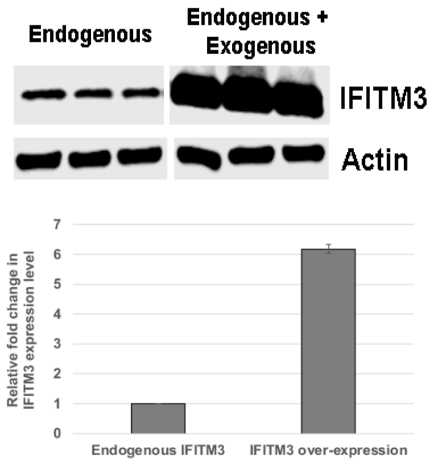

(d)

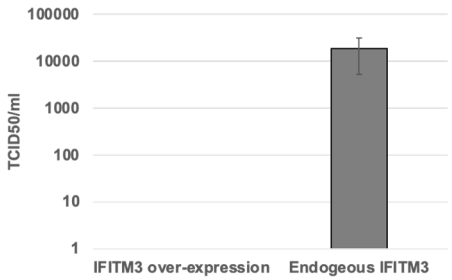

Figure 3. IFITM3 expression level is inversely correlated to PRRSV replication efficiency. (a) IFN-alpha induces IFITM3 expression. Relative fold changes in IFITM3 and Mx1 gene expression in PRRSV 23983 infected groups

 doi:10.20944/preprints202506.0696.v1

when compared to mock treated groups are shown. More abundant Mx1 as compared to IFITM3 mRNA is induced by IFN-alpha. Representative data show the average and standard deviation of three replicates. (b) IFN-alpha inhibits PRRSV infection in a dose-dependent manner. Real-time RT-PCR shows the relative fold changes of IFITM3 and PRRSV N mRNA gene expression in IFN-alpha treated groups at different concentrations when compared to non-treated control groups. Representative data show the average of two replicates. (c) Over-expression of IFITM3 results in 6.2-fold increase in total IFITM3 protein level compared to endogenous IFITM3 expression level. (d) No virus titer was detected in cells over-expressing IFITM3 while $1.9x10^4$ $TCID_{50}$ titer was detected in cells only expressing endogenous level of IFITM3.

3.4. Amphotericin B Partially Restores PRRSV Replication in IFITM3 Overexpressing Cells

IFITM3 overexpression significantly reduced PRRSV infection in MARC-145 cells (Figure 4a). To quantitatively estimate the PRRSV infection in the Amphotericin B treated and untreated group, flow cytometry was performed. Analysis of virus-infected cells in the presence or absence of Amphotericin B treatment confirmed that Amphotericin B partially restored the replication of PRRSV in cells over-expressing IFITM3 (Figure 4b). In the Amphotericin B untreated group, a significant reduction in mean fluorescence intensity ($p < 0.05$) in the IFITM3 overexpressing cells as compared to vector control was observed (Figure 4b). This data further validates our observation shown in Figure 1.

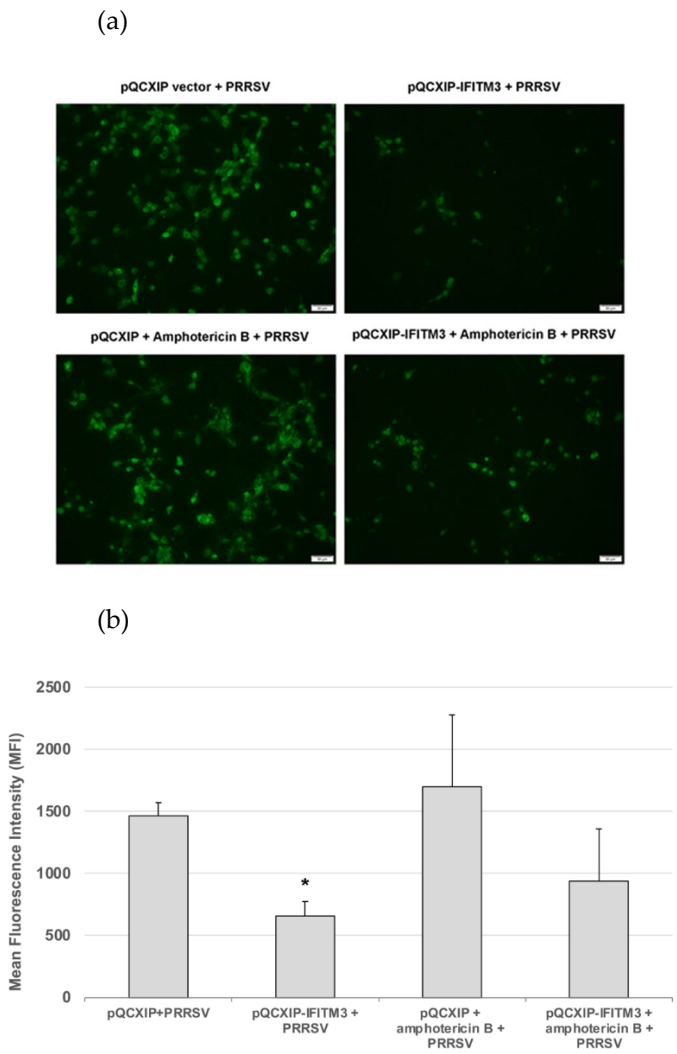

Figure 4. Amphotericin B treatment only partially restores PRRSV replication in cells over-expressing IFITM3. (a) Immunofluorescence staining of virus-infected cells in the presence or absence of amphotericin B treatment. Images were captured at 10x magnification. (b) Flow cytometry analysis of virus-infected cells in the presence or absence of Amphotericin B. * indicates $p < 0.05$ when compared to the pQCXIP + PRRSV group.

 doi:10.20944/preprints202506.0696.v1

3.5. Colocalization of PRRSV with Early and Late Endosome/Lysosome Markers at 3 hpi

To examine whether PPRSV enters the late endosomes, MARC-145 cells infected with PRRSV 23983 for 1 h, 3 h, or 6 h were stained for either the early endosomal marker, EEA1 or late endosome/lysosome marker, LAMP-1. While approximately 38% colocalization between PRRSV and EEA1 was observed at 3 hpi (Figure 5a,b), only 12% colocalization between PRRSV and LAMP-1 was observed at 3 h after virus infection (Figure 5c,d). Few colocalizations between PRRSV and EEA1 or LAMP1 were observed at 1 and 6 hpi (Figure 5).

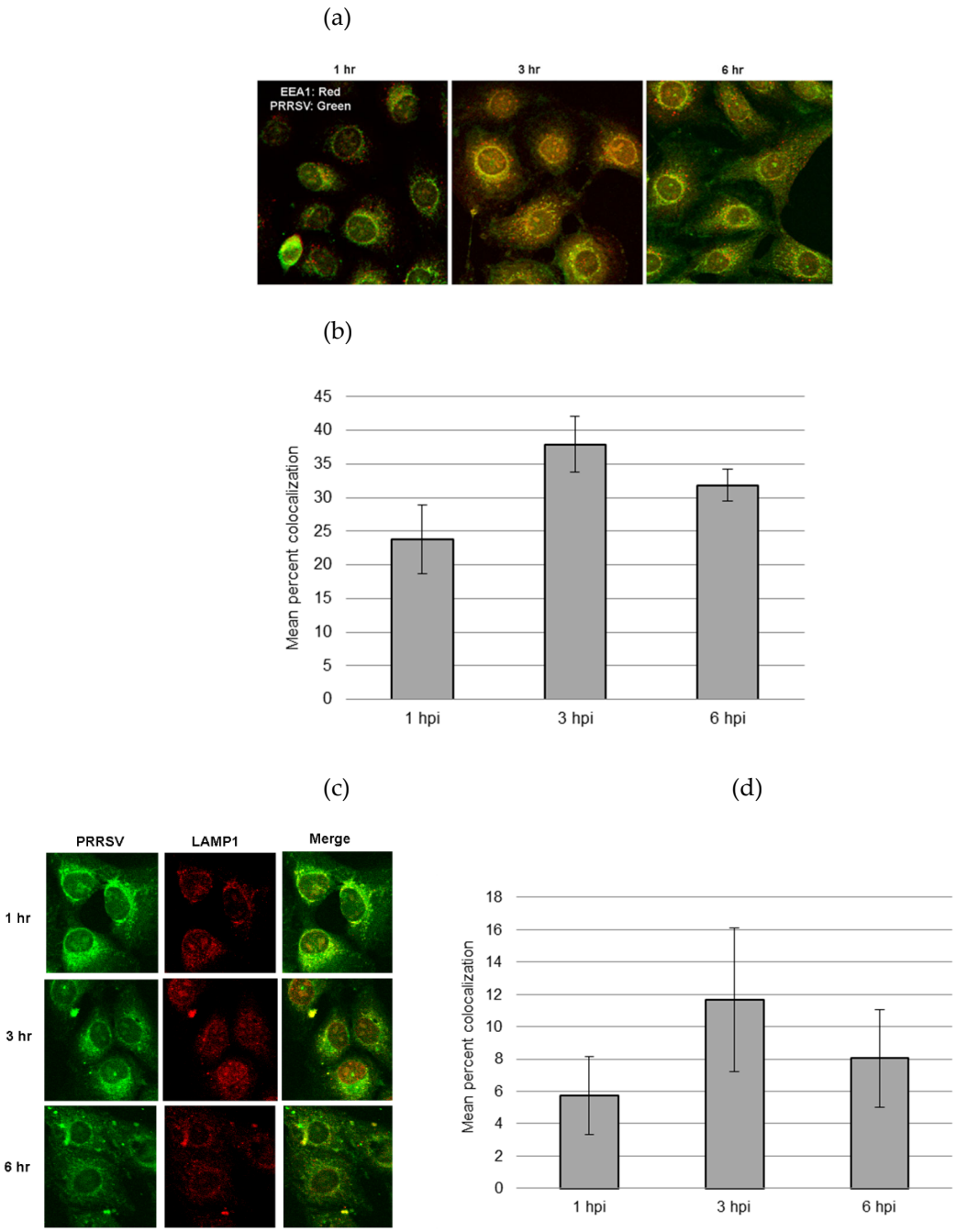

Figure 5. Colocalization of PRRSV with early endosome marker EEA1 and late endosome marker LAMP1 at 1, 3, and 6 h after virus infection. (a) Colocalization of PRRSV with EEA1 at different time points. (b) Mean percent colocalization was estimated by manual thresholding using Image J. For each time point, mean percent colocalization was calculated by randomly selecting five cells for each microscopic field. Greater percentage of colocalization occurred with EEA1 at 3 hpi as compared to 1 or 6 hpi. (c) Colocalization of PRRSV with LAMP-1 at different time points. (d) Only limited colocalization between PRRSV and late endosome/lysosome marker

 doi:10.20944/preprints202506.0696.v1

LAMP1 was observed at 3 h after virus infection. Images were captured using a confocal microscope at 40x magnification.

3.6. Over-Expression of IFITM3 Does Not Significantly Impact Virus Entry

Cells over-expressing exogenous IFITM3 were stained for PRRSV at 3 and 24 hpi. Colocalization of IFITM3 with PRRSV was observed at both time points (Figure 6a). An average 73% of IFITM3 expressing cells contained virus at 3 hpi, while only approximately 27% of IFITM3 expressing cells contained virus at 24 hpi (Figure 6b). Confocal images of control vector transfected cells showed clusters of virus-infected cells at 24 hpi (data not shown), indicative of efficient cell-cell spread of virus. In contrast, IFITM3 over-expressing cells typically showed a few punctuate positive virus staining within isolated individual cells at 24 hpi (Figure 6a).

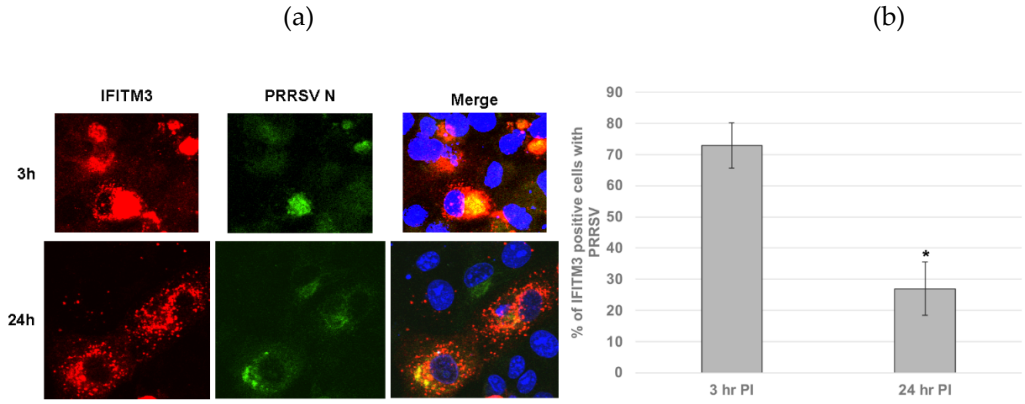

Figure 6. Over-expression of IFITM3 does not significantly impact virus entry. (a) Cells over-expressing exogenous IFITM3 contains PRRSV at 3 and 24 hpi. Colocalization of PRRSV with overexpressed IFITM3 was observed (yellow arrows). Red: IFITM3; Green: PRRSV N; Blue: DAPI. Images were taken at 40x magnification. (b) The percentage of PRRSV positive cells was significantly lower ($p < 0.0001$) in IFITM3 transfected cells at 24 hpi than that at 3 hpi. Quantification was done by counting PRRSV positive cells and IFITM3-HA expressing cells obtained from five different microscopic fields.

3.7. Over-Expression of IFITM3 Reduces the Level of p-Akt and Increases the Ratios of LC3-II/LC3-I

To examine whether IFITM3 over-expression affect the level of p-Akt and the ratios of LC3-II/LC3-I, we performed western blot analysis. As shown in Figure 7, IFITM3 over-expression reduced the level of p-Akt by approximately 50% compared to vector control transfected cells. Furthermore, a significant decrease ($p < 0.05$) in p-Akt level was observed in PRRSV-infected cells over-expressing IFITM3 compared to PRRSV-infected cells transfected with vector control. Approximately 65% reduction in p-Akt was observed in PRRSV-infected cells over-expressing IFITM3 compared to PRRSV-infected cells transfected with vector control (Figure 7).

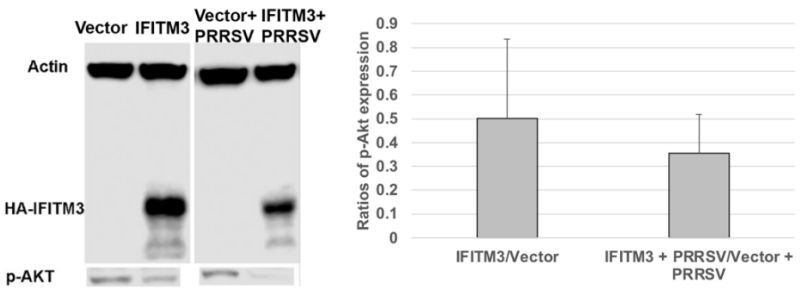

Figure 7. Over-expression of IFITM3 reduce the level of phosphorylated Akt by 50% compared to vector control. A representative western blot image shows the expression level of p-Akt. The averages and standard deviations

 doi:10.20944/preprints202506.0696.v1

of three replicates are shown in the graph. A significant decrease in the level of p-Akt was observed in IFITM3 over-expressing and PRRSV infected cells compared to vector transfected and PRRSV infected cells ($p < 0.05$).

Similarly, a slightly increased LC3II/LC3-I ratio was observed in IFITM3 over-expressing cells compared to vector control cells (Figure 8). A slight decrease in LC3II/LC3-I ratio was observed in PRRSV-infected cells over-expressing IFITM3 than PRRSV-infected cells transfected with vector control (Figure 8). PRRSV infection, vector control transfection as well as IFITM3 over-expression all induced a significantly higher ratio of LC3-II/LC3-I than mock cells ($p < 0.05$).

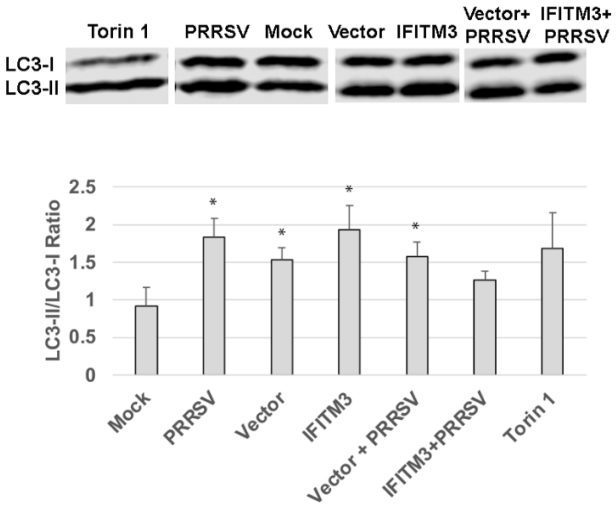

Figure 8. Over-expression of IFITM3 increases the ratio of LC3-II/LC3-I by 128% compared to vector control. A representative western blot image shows the expression level of LC3-I and LC3-II. The averages and standard deviations of three replicates are shown in the graph. * Indicates significant differences compared to mock ($p < 0.05$).

4. Discussion

IFITM3 is an interferon induced antiviral gene and partly contributes to the antiviral effect of interferon. Indeed, IFITM3 has been shown to restrict the replication of a diverse array of enveloped RNA viruses including PRRSV [2,15,30]. We have shown here that over-expression of IFITM3 reduced PRRSV replication in MARC-145 cells, which is consistent with the previous observation made by others [23]. Similarly, silencing of IFITM3 enhanced PRRSV replication as shown by both our study and Zhang, et al. [23]. The observed virus replication enhancement effect in our study is lower than what has been described previously [23], which could be due to the relatively low knockdown efficiency (an average of 50%) and high MOI of virus used in our study. This is supported by the recent report showing that IFITM3 is effective in restricting lower threshold of virus infection [31]. Collectively, both overexpression and RNA silencing of IFITM3 data suggest its antiviral effect against PRRSV.

IFITM3 is constitutively expressed in both MARC-145 cells and porcine alveolar macrophages (PAMs). Our study and others [23] have shown upregulation of IFITM3 protein upon IFN-α treatment, which is positively correlated with reduced PRRSV replication. PRRSV upregulated IFITM3 expression in PAMs at 24 hpi [23]. Interestingly, we observed that PRRSV infection reduced IFITM3 gene expression in MARC-145 cells at 24 hpi. This discrepancy could be due to different cell types used in each study.

It is generally believed that IFITM3 decreases membrane fluidity thereby inhibiting virus-cell membrane fusion and cytosolic release [6]. Studies using single virus fusion assay have shown that IFITM3 restricts virus membrane fusion [32,33]. One earlier study reported that PRRSV is associated with early endosome only and not late endosomes [22]. Similarly, we found that very few PRRSV colocalized with LAMP-1, a marker of late endosome and lysosome, during the first 6 hpi. PRRSV

 doi:10.20944/preprints202506.0696.v1

colocalized with the early endosome marker EEA1 at 3 hpi, but most disappeared from early endosome at 6 hpi. IFITM3 is known to restrict virus membrane fusion and trap virus in late endosome for degradation [24,34]. Amphotericin B treatment has been shown to restore infection of many viruses that are restricted by IFITM3 [33,35]. In a recent study, Amphotericin B reversed the IFITM3 mediated entry-restriction of several pseudovirus particles tested, including SARS-CoVpp and IAVpp, but not LASVpp [36]. Amphotericin B is an antifungal drug known to restore membrane fluidity thereby reversing the effect of IFITM3 mediated virus restriction [35]. It forms leak ion channels in the cell membrane and has also been shown to associate with cholesterol in lipid rafts [24]. Our observation suggests that IFITM3 may restrict PRRSV in a mechanism different from SARS-CoV and IAV [36] since only 12% of virus was detected in late endosome. This observation is also consistent with our data showing that Amphotericin B treatment only partially restores PRRSV replication. Interestingly, Zhang et al. has shown that PRRSV colocalizes not only with early endosomes but also late endosomes/lysosomes [23]. The discrepant results could be due to different experimental conditions used in each study. Zhang et al. has also shown that IFITM3 does not restrict PRRSV attachment, entry, and internalization into endosomes, but inhibits virus membrane fusion via cholesterol induction in cellular vesicles [23].

Suddala et al. showed that IFITM3 expressing cells are not infected by IAV at 12 hpi, but adjacent cells not expressing IFITM3 are infected, suggesting that this antiviral activity of IFITM3 is not due to conditioned medium [37]. Our results showed that IFITM3 expressing cells do contain PRRSV at both 3h and 24 h pi, suggesting that a potential different mechanism mediates the antiviral activity to PRRSV than IAV. Suddala et al. suggest that IFITM3 accumulation at the sites of virus fusion prevent virus release into cytoplasm and replication [37]. We observed an average 73% of IFITM3 expressing cell contains PRRSV at 3 hpi, indicating that over-expression of IFITM3 has little effect on virus entry. However, at 24 hpi, only 27% of IFITM3 expressing cells contained PRRSV. Our study also showed that PRRSV in IFITM3 overexpressing MARC-145 cells exhibited a punctuated staining pattern in isolated individual cells at 24 hpi, while vector control cells typically showed clusters of virus positive cells (data not shown and Figure 4a). These observations suggest that efficient cell-cell spread of virus may be affected by over-expression of IFITM3, which has also been shown by Zhang et al. [23]. Earlier studies have shown that PRRSV upregulates the formation of tunneling nanotubes (TNTs) to facilitate the intercellular spread of PRRSV [38]. Hence it is tempting to speculate that IFITM3 over-expression may affect cellular spread of virus by limiting formation of TNTs. Further studies are needed to uncover the impact of IFITM3 overexpression on formation of TNT upon PRRSV infection. Overall, our data support a role of IFITM3 in restricting PRRSV post-entry into cells.

Phosphatidylinositol 3-kinase (PI3K)-dependent Akt signaling pathway is involved in cell survival, cell proliferation, and differentiation. The pro-viral effect of PI3K/Akt pathway on the replication of many viruses including PRRSV has been reported previously [39]. It is reasonable to speculate that the reduced p-Akt level in IFITM3 over-expressing cells may also partially contribute to the reduced virus replication observed here. It has been reported that over-expression of IFITM3 or other ISGs such as GBP1 can induce autophagy [40,41], which may restrict virus replication [40]. An increased LC3-II/LC3-I ratio in IFITM3 over-expressing MARC-145 cells than vector control cells may also partially contribute to the reduced PRRSV replication. In a separate study, we have observed that over-expression of IFITM3 in H1299 cells induced autophagy and enhanced Seneca virus A replication [42]. Akt is known to regulate autophagy [43], which is supported by our observation showing the correlation between p-Akt and autophagy marker (LC3-II/LC3-I ratio). Interestingly, several previous studies reported that autophagy sustained or enhanced PRRSV replication [43–45]. Autophagy can serve as a double-edged sword during virus infections [46]. Future studies are needed to examine the role of cellular changes due to the non-physiological level of IFITM3 over-expression and their contribution to the replication efficiency of other viruses in different cell types.

 doi:10.20944/preprints202506.0696.v1

5. Conclusions

In conclusion, over-expression of IFITM3 reduced PRRSV infection and may restrict PRRSV at the post-entry steps since amphotericin B treatment did not completely rescue PRRSV infection. Silencing of endogenous IFITM3 increased PRRSV RNA copies and virus titers. Furthermore, an inverse correlation between IFITM3 level and PRRSV gene copies was observed. Further study is needed to better understand the mechanisms by which IFITM3 restricts PRRSV replication in MARC-145 cells and porcine alveolar mac-rophages (PAMs).

Supplementary Materials: Not applicable.

Author Contributions: Conceptualization, X.W.; methodology, P.K., S.A. and X.W.; formal analysis, P.K., X.W. and M.H.; investigation, P.K., S.A. and X.W.; resources, X.W., E.N. and S.L.; writing—original draft preparation, P.K. and X.W.; writing—review and editing, X.W. and P.K.; visualization and supervision, X.W.; funding acquisition, X.W.

Funding: This research was funded by the Animal Health Program (grant #2021-67016-34460) from the USDA National Institute of Food and Agriculture (NIFA), USDA NIFA Hatch (grant #1000514), Hatch Multi State (grant #1010908), and South Dakota Agricultural Experiment Station.

Institutional Review Board Statement: Not applicable.

Informed Consent Statement: Not applicable.

Data Availability Statement: Data is contained within the article.

Acknowledgments: This material is based upon work conducted using the South Dakota State University Functional Genomics Core Facility (RRID:SCR_023786) supported in part by the National Science Foundation/EPSCoR Grant No. 0091948, the South Dakota Agricultural Experiment Station, and by the State of South Dakota. Research reported in this publication was supported by the National Institute of General Medical Sciences of the National Institutes of Health under Award Number P20GM135008. The content is solely the responsibility of the authors and does not necessarily represent the official views of the National Institutes of Health. The authors also thank Dr. Liping Gu at the Functional Genomics Core Facility, South Dakota State University for her technical assistance.

Conflicts of Interest: The authors declare no conflicts of interest.

Abbreviations.

The following abbreviations are used in this manuscript:

IFITM3	Interferon induced transmembrane protein 3
PRRSV	Porcine reproductive and respiratory syndrome virus
ISGs	Interferon stimulated genes
ZMPSTE24	Zinc metallopeptidase STE24
IAV	Influenza A virus
MEFs	Mouse embryonic fibroblasts
vRNPs	Viral ribonucleoproteins
SARS-CoV	Severe acute respiratory syndrome coronavirus
LASVpp	Lassa virus pseudovirus
PI3K	Phosphatidylinositol 3-kinase
GBP1	Guanylate binding protein 1

 doi:10.20944/preprints202506.0696.v1

TNTs	Tunneling nanotubes

References

1. Schneider, W.M.; Chevillotte, M.D.; Rice, C.M. Interferon-Stimulated Genes: A Complex Web of Host Defenses. *Annu. Rev. Immunol.* 2014, *32*, 513–545.
2. Feeley, E.M.; Sims, J.S.; John, S.P.; Chin, C.R.; Pertel, T.; Chen, L.-M.; Gaiha, G.D.; Ryan, B.J.; Donis, R.O.; Elledge, S.J.; et al. IFITM3 Inhibits Influenza A Virus Infection by Preventing Cytosolic Entry. *PLoS Pathog.* **2011**, *7*, e1002337, doi:10.1371/journal.ppat.1002337.
3. Friedman, R.L.; Manly, S.P.; McMahon, M.; Kerr, I.M.; Stark, G.R. Transcriptional and Posttranscriptional Regulation of Interferon-Induced Gene Expression in Human Cells. *Cell* **1984**, *38*, 745–755, doi:10.1016/0092-8674(84)90270-8.
4. Bailey, C.C.; Zhong, G.; Huang, I.-C.; Farzan, M. IFITM-Family Proteins: The Cell's First Line of Antiviral Defense. *Annu. Rev. Virol.* **2014**, *1*, 261–283, doi:10.1146/annurev-virology-031413-085537.
5. Brass, A.L.; Huang, I.-C.; Benita, Y.; John, S.P.; Krishnan, M.N.; Feeley, E.M.; Ryan, B.J.; Weyer, J.L.; van der Weyden, L.; Fikrig, E.; et al. The IFITM Proteins Mediate Cellular Resistance to Influenza A H1N1 Virus, West Nile Virus, and Dengue Virus. *Cell* **2009**, *139*, 1243–1254, doi:10.1016/j.cell.2009.12.017.
6. Perreira, J.M.; Chin, C.R.; Feeley, E.M.; Brass, A.L. IFITMs Restrict the Replication of Multiple Pathogenic Viruses. *J. Mol. Biol.* **2013**, *425*, 4937–4955, doi:10.1016/j.jmb.2013.09.024.
7. Haller, O.; Kochs, G. Human MxA Protein: An Interferon-Induced Dynamin-like GTPase with Broad Antiviral Activity. *J. Interferon Cytokine Res. Off. J. Int. Soc. Interferon Cytokine Res.* **2011**, *31*, 79–87, doi:10.1089/jir.2010.0076.
8. Okumura, F.; Okumura, A.J.; Uematsu, K.; Hatakeyama, S.; Zhang, D.-E.; Kamura, T. Activation of Double-Stranded RNA-Activated Protein Kinase (PKR) by Interferon-Stimulated Gene 15 (ISG15) Modification down-Regulates Protein Translation. *J. Biol. Chem.* **2013**, *288*, 2839–2847, doi:10.1074/jbc.M112.401851.
9. Schoggins, J.W.; Rice, C.M. Interferon-Stimulated Genes and Their Antiviral Effector Functions. *Curr. Opin. Virol.* **2011**, *1*, 519–525, doi:10.1016/j.coviro.2011.10.008.
10. Bailey, C.C.; Huang, I.-C.; Kam, C.; Farzan, M. Ifitm3 Limits the Severity of Acute Influenza in Mice. *PLoS Pathog.* **2012**, *8*, e1002909, doi:10.1371/journal.ppat.1002909.
11. Brass, A.L.; Huang, I.-C.; Benita, Y.; John, S.P.; Krishnan, M.N.; Feeley, E.M.; Ryan, B.J.; Weyer, J.L.; van der Weyden, L.; Fikrig, E.; et al. The IFITM Proteins Mediate Cellular Resistance to Influenza A H1N1 Virus, West Nile Virus, and Dengue Virus. *Cell* **2009**, *139*, 1243–1254, doi:10.1016/j.cell.2009.12.017.
12. Smith, S.; Weston, S.; Kellam, P.; Marsh, M. IFITM Proteins-Cellular Inhibitors of Viral Entry. *Curr. Opin. Virol.* **2014**, *4*, 71–77, doi:10.1016/j.coviro.2013.11.004.
13. Gorman, M.J.; Poddar, S.; Farzan, M.; Diamond, M.S. The Interferon-Stimulated Gene Ifitm3 Restricts West Nile Virus Infection and Pathogenesis. *J. Virol.* **2016**, *90*, 8212–8225, doi:10.1128/JVI.00581-16.
14. Weidner, J.M.; Jiang, D.; Pan, X.-B.; Chang, J.; Block, T.M.; Guo, J.-T. Interferon-Induced Cell Membrane Proteins, IFITM3 and Tetherin, Inhibit Vesicular Stomatitis Virus Infection via Distinct Mechanisms. *J. Virol.* **2010**, *84*, 12646–12657, doi:10.1128/JVI.01328-10.
15. Savidis, G.; Perreira, J.M.; Portmann, J.M.; Meraner, P.; Guo, Z.; Green, S.; Brass, A.L. The IFITMs Inhibit Zika Virus Replication. *Cell Rep.* **2016**, *15*, 2323–2330, doi:10.1016/j.celrep.2016.05.074.
16. Done, S.H.; Paton, D.J.; White, M.E. Porcine Reproductive and Respiratory Syndrome (PRRS): A Review, with Emphasis on Pathological, Virological and Diagnostic Aspects. *Br. Vet. J.* **1996**, *152*, 153–174, doi:10.1016/s0007-1935(96)80071-6.
17. Nauwynck, H.J.; Duan, X.; Favoreel, H.W.; Van Oostveldt, P.; Pensaert, M.B. Entry of Porcine Reproductive and Respiratory Syndrome Virus into Porcine Alveolar Macrophages via Receptor-Mediated Endocytosis. *J. Gen. Virol.* **1999**, *80 (Pt 2)*, 297–305, doi:10.1099/0022-1317-80-2-297.
18. Zhang, Q.; Yoo, D. PRRS Virus Receptors and Their Role for Pathogenesis. *Vet. Microbiol.* **2015**, *177*, 229–241, doi:10.1016/j.vetmic.2015.04.002.

 doi:10.20944/preprints202506.0696.v1

19. Calvert, J.G.; Slade, D.E.; Shields, S.L.; Jolie, R.; Mannan, R.M.; Ankenbauer, R.G.; Welch, S.-K.W. CD163 Expression Confers Susceptibility to Porcine Reproductive and Respiratory Syndrome Viruses. *J. Virol.* **2007**, *81*, 7371–7379, doi:10.1128/JVI.00513-07.
20. Welch, S.-K.W.; Calvert, J.G. A Brief Review of CD163 and Its Role in PRRSV Infection. *Virus Res.* **2010**, *154*, 98–103, doi:10.1016/j.virusres.2010.07.018.
21. Kreutz, L.C.; Ackermann, M.R. Porcine Reproductive and Respiratory Syndrome Virus Enters Cells through a Low pH-Dependent Endocytic Pathway. *Virus Res.* **1996**, *42*, 137–147, doi:10.1016/0168-1702(96)01313-5.
22. Van Gorp, H.; Van Breedam, W.; Delputte, P.L.; Nauwynck, H.J. The Porcine Reproductive and Respiratory Syndrome Virus Requires Trafficking through CD163-Positive Early Endosomes, but Not Late Endosomes, for Productive Infection. *Arch. Virol.* **2009**, *154*, 1939–1943, doi:10.1007/s00705-009-0527-1.
23. Zhang, A.; Duan, H.; Zhao, H.; Liao, H.; Du, Y.; Li, L.; Jiang, D.; Wan, B.; Wu, Y.; Ji, P.; et al. Interferon-Induced Transmembrane Protein 3 Is a Virus-Associated Protein Which Suppresses Porcine Reproductive and Respiratory Syndrome Virus Replication by Blocking Viral Membrane Fusion. *J. Virol.* **2020**, *94*, doi:10.1128/JVI.01350-20.
24. Waheed, A.A.; Ablan, S.D.; Soheilian, F.; Nagashima, K.; Ono, A.; Schaffner, C.P.; Freed, E.O. Inhibition of Human Immunodeficiency Virus Type 1 Assembly and Release by the Cholesterol-Binding Compound Amphotericin B Methyl Ester: Evidence for Vpu Dependence. *J. Virol.* **2008**, *82*, 9776–9781, doi:10.1128/JVI.00917-08.
25. Katwal, P.; Aftab, S.; Nelson, E.; Hildreth, M.; Li, S.; Wang, X. Role of Zinc Metalloprotease (ZMPSTE24) in Porcine Reproductive and Respiratory Syndrome Virus (PRRSV) Replication in Vitro. *Arch. Virol.* **2022**, *167*, 2281–2286, doi:10.1007/s00705-022-05529-0.
26. Fu, B.; Wang, L.; Li, S.; Dorf, M.E. ZMPSTE24 Defends against Influenza and Other Pathogenic Viruses. *J. Exp. Med.* **2017**, *214*, 919–929, doi:10.1084/jem.20161270.
27. Nelson, E.A.; Christopher-Hennings, J.; Drew, T.; Wensvoort, G.; Collins, J.E.; Benfield, D.A. Differentiation of U.S. and European Isolates of Porcine Reproductive and Respiratory Syndrome Virus by Monoclonal Antibodies. *J. Clin. Microbiol.* **1993**, *31*, 3184–3189, doi:10.1128/jcm.31.12.3184-3189.1993.
28. Schindelin, J.; Arganda-Carreras, I.; Frise, E.; Kaynig, V.; Longair, M.; Pietzsch, T.; Preibisch, S.; Rueden, C.; Saalfeld, S.; Schmid, B.; et al. Fiji: An Open-Source Platform for Biological-Image Analysis. *Nat. Methods* **2012**, *9*, 676–682, doi:10.1038/nmeth.2019.
29. Livak, K.J.; Schmittgen, T.D. Analysis of Relative Gene Expression Data Using Real-Time Quantitative PCR and the 2(-Delta Delta C(T)) Method. *Methods San Diego Calif* **2001**, *25*, 402–408, doi:10.1006/meth.2001.1262.
30. Franz, S.; Pott, F.; Zillinger, T.; Schüler, C.; Dapa, S.; Fischer, C.; Passos, V.; Stenzel, S.; Chen, F.; Döhner, K.; et al. Human IFITM3 Restricts Chikungunya Virus and Mayaro Virus Infection and Is Susceptible to Virus-Mediated Counteraction. *Life Sci. Alliance* **2021**, *4*, doi:10.26508/lsa.202000909.
31. Denz, P.J.; Speaks, S.; Kenney, A.D.; Eddy, A.C.; Papa, J.L.; Roettger, J.; Scace, S.C.; Rubrum, A.; Hemann, E.A.; Forero, A.; et al. Innate Immune Control of Influenza Virus Interspecies Adaptation via IFITM3. *Nat. Commun.* **2024**, *15*, 9375, doi:10.1038/s41467-024-53792-3.
32. Desai, T.M.; Marin, M.; Chin, C.R.; Savidis, G.; Brass, A.L.; Melikyan, G.B. IFITM3 Restricts Influenza A Virus Entry by Blocking the Formation of Fusion Pores Following Virus-Endosome Hemifusion. *PLoS Pathog.* **2014**, *10*, e1004048, doi:10.1371/journal.ppat.1004048.
33. McMichael, T.M.; Zhang, Y.; Kenney, A.D.; Zhang, L.; Zani, A.; Lu, M.; Chemudupati, M.; Li, J.; Yount, J.S. IFITM3 Restricts Human Metapneumovirus Infection. *J. Infect. Dis.* **2018**, *218*, 1582–1591, doi:10.1093/infdis/jiy361.
34. Amini-Bavil-Olyaee, S.; Choi, Y.J.; Lee, J.H.; Shi, M.; Huang, I.-C.; Farzan, M.; Jung, J.U. The Antiviral Effector IFITM3 Disrupts Intracellular Cholesterol Homeostasis to Block Viral Entry. *Cell Host Microbe* **2013**, *13*, 452–464, doi:10.1016/j.chom.2013.03.006.
35. Lin, T.-Y.; Chin, C.R.; Everitt, A.R.; Clare, S.; Perreira, J.M.; Savidis, G.; Aker, A.M.; John, S.P.; Sarlah, D.; Carreira, E.M.; et al. Amphotericin B Increases Influenza A Virus Infection by Preventing IFITM3-Mediated Restriction. *Cell Rep.* **2013**, *5*, 895–908, doi:10.1016/j.celrep.2013.10.033.

 doi:10.20944/preprints202506.0696.v1

36. Zhao, X.; Zheng, S.; Chen, D.; Zheng, M.; Li, X.; Li, G.; Lin, H.; Chang, J.; Zeng, H.; Guo, J.-T. LY6E Restricts Entry of Human Coronaviruses, Including Currently Pandemic SARS-CoV-2. *J. Virol.* **2020**, *94*, doi:10.1128/JVI.00562-20.
37. Suddala, K.C.; Lee, C.C.; Meraner, P.; Marin, M.; Markosyan, R.M.; Desai, T.M.; Cohen, F.S.; Brass, A.L.; Melikyan, G.B. Interferon-Induced Transmembrane Protein 3 Blocks Fusion of Sensitive but Not Resistant Viruses by Partitioning into Virus-Carrying Endosomes. *PLoS Pathog.* **2019**, *15*, e1007532, doi:10.1371/journal.ppat.1007532.
38. Guo, R.; Katz, B.B.; Tomich, J.M.; Gallagher, T.; Fang, Y. Porcine Reproductive and Respiratory Syndrome Virus Utilizes Nanotubes for Intercellular Spread. *J. Virol.* **2016**, *90*, 5163–5175, doi:10.1128/JVI.00036-16.
39. Wang, X.; Zhang, H.; Abel, A.M.; Young, A.J.; Xie, L.; Xie, Z. Role of Phosphatidylinositol 3-Kinase (PI3K) and Akt1 Kinase in Porcine Reproductive and Respiratory Syndrome Virus (PRRSV) Replication. *Arch. Virol.* **2014**, *159*, 2091–2096, doi:10.1007/s00705-014-2016-4.
40. Gu, T.; Yu, D.; Xu, L.; Yao, Y.-L.; Yao, Y.-G. Tupaia GBP1 Interacts with STING to Initiate Autophagy and Restrict Herpes Simplex Virus Type 1 Infection. *J. Immunol. Baltim. Md 1950* **2021**, *207*, 2673–2680, doi:10.4049/jimmunol.2100325.
41. Yount, J.S.; Karssemeijer, R.A.; Hang, H.C. S-Palmitoylation and Ubiquitination Differentially Regulate Interferon-Induced Transmembrane Protein 3 (IFITM3)-Mediated Resistance to Influenza Virus. *J. Biol. Chem.* **2012**, *287*, 19631–19641, doi:10.1074/jbc.M112.362095.
42. Aftab, S.; Nelson, E.; Hildreth, M.; Wang, X. Silencing RNA-Mediated Knockdown of IFITM3 Enhances Senecavirus A Replication. *Pathogens* **2024**, *13*, doi:10.3390/pathogens13040290.
43. Noguchi, M.; Hirata, N.; Suizu, F. The Links between AKT and Two Intracellular Proteolytic Cascades: Ubiquitination and Autophagy. *Biochim. Biophys. Acta* **2014**, *1846*, 342–352, doi:10.1016/j.bbcan.2014.07.013.
44. Chen, Q.; Fang, L.; Wang, D.; Wang, S.; Li, P.; Li, M.; Luo, R.; Chen, H.; Xiao, S. Induction of Autophagy Enhances Porcine Reproductive and Respiratory Syndrome Virus Replication. *Virus Res.* **2012**, *163*, 650–655, doi:10.1016/j.virusres.2011.11.008.
45. Chen, Q.; Men, Y.; Wang, D.; Xu, D.; Liu, S.; Xiao, S.; Fang, L. Porcine Reproductive and Respiratory Syndrome Virus Infection Induces Endoplasmic Reticulum Stress, Facilitates Virus Replication, and Contributes to Autophagy and Apoptosis. *Sci. Rep.* **2020**, *10*, 13131, doi:10.1038/s41598-020-69959-z.
46. Liu, Q.; Qin, Y.; Zhou, L.; Kou, Q.; Guo, X.; Ge, X.; Yang, H.; Hu, H. Autophagy Sustains the Replication of Porcine Reproductive and Respiratory Virus in Host Cells. *Virology* **2012**, *429*, 136–147, doi:10.1016/j.virol.2012.03.022.
47. Choi, Y.; Bowman, J.W.; Jung, J.U. Autophagy during Viral Infection - a Double-Edged Sword. *Nat. Rev. Microbiol.* **2018**, *16*, 341–354, doi:10.1038/s41579-018-0003-6.